EAPS 53600: Introduction to General Circulation of the Atmosphere
Spring 2020
Prof. Dan Chavas

NASA GEOS-5 Computer Model

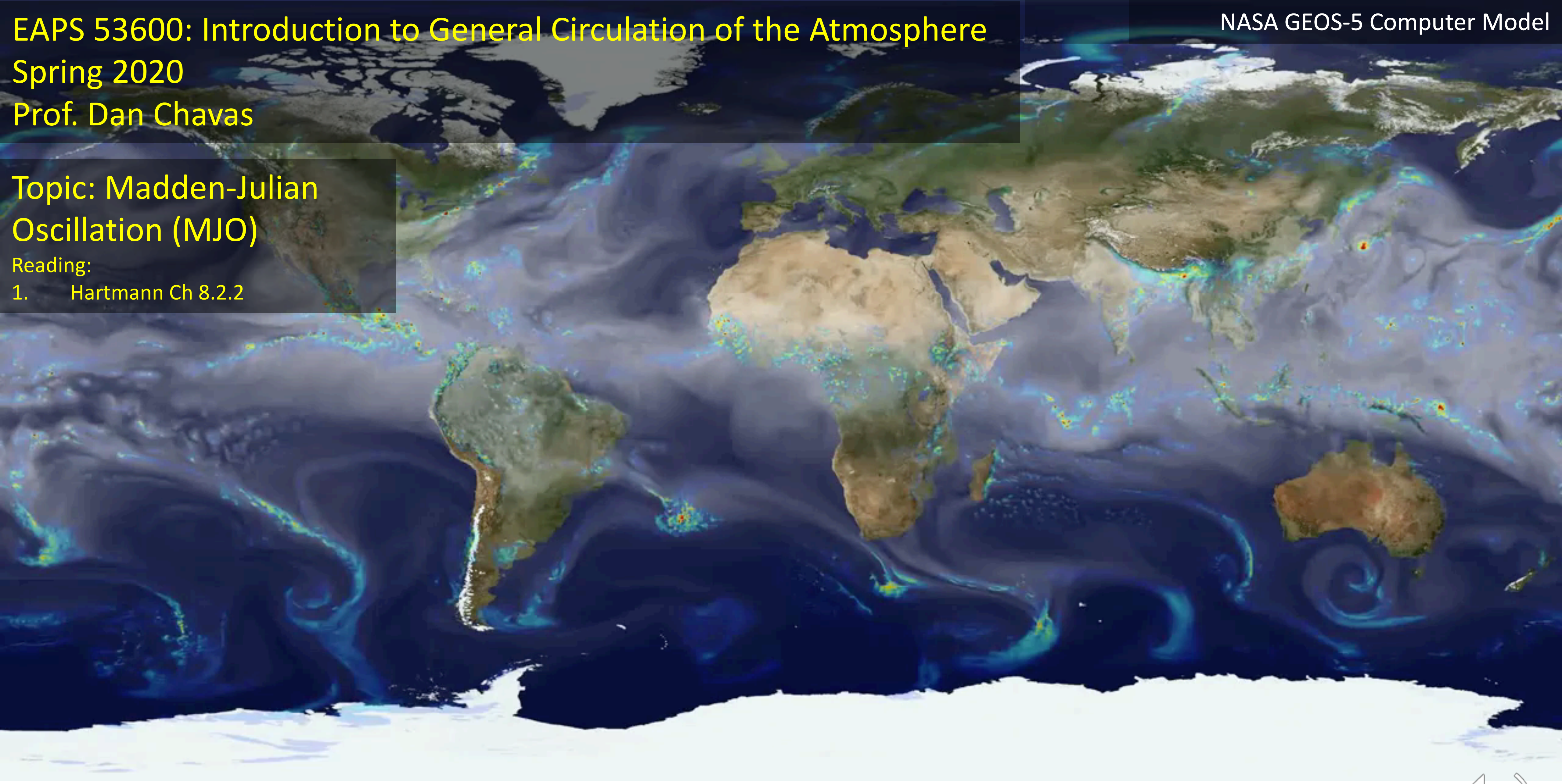

Topic: Madden-Julian Oscillation (MJO)

Reading:

1. Hartmann Ch 8.2.2

White: total precipitable water (brigher white = more water vapor in column)

Colors: precipitation rate ($0 - 15\frac{mm}{hr}$, red=highest)

Source: https://svs.gsfc.nasa.gov/cgi-bin/details.cgi?aid=30017

Learning outcomes for today:

- **Describe what the Madden-Julian Oscillation is and how to identify it**
- **Explain why it exists**
- **Explain what causes it to propagate eastward**

Madden Julian Oscillation (MJO) Basics

https://www.youtube.com/watch?v=UsWHHE_jkGE https://www.youtube.com/watch?v=V3HE7WMm-KM

Duration: $\tau \sim 1-2$ months
Frequency: $1-2$ months

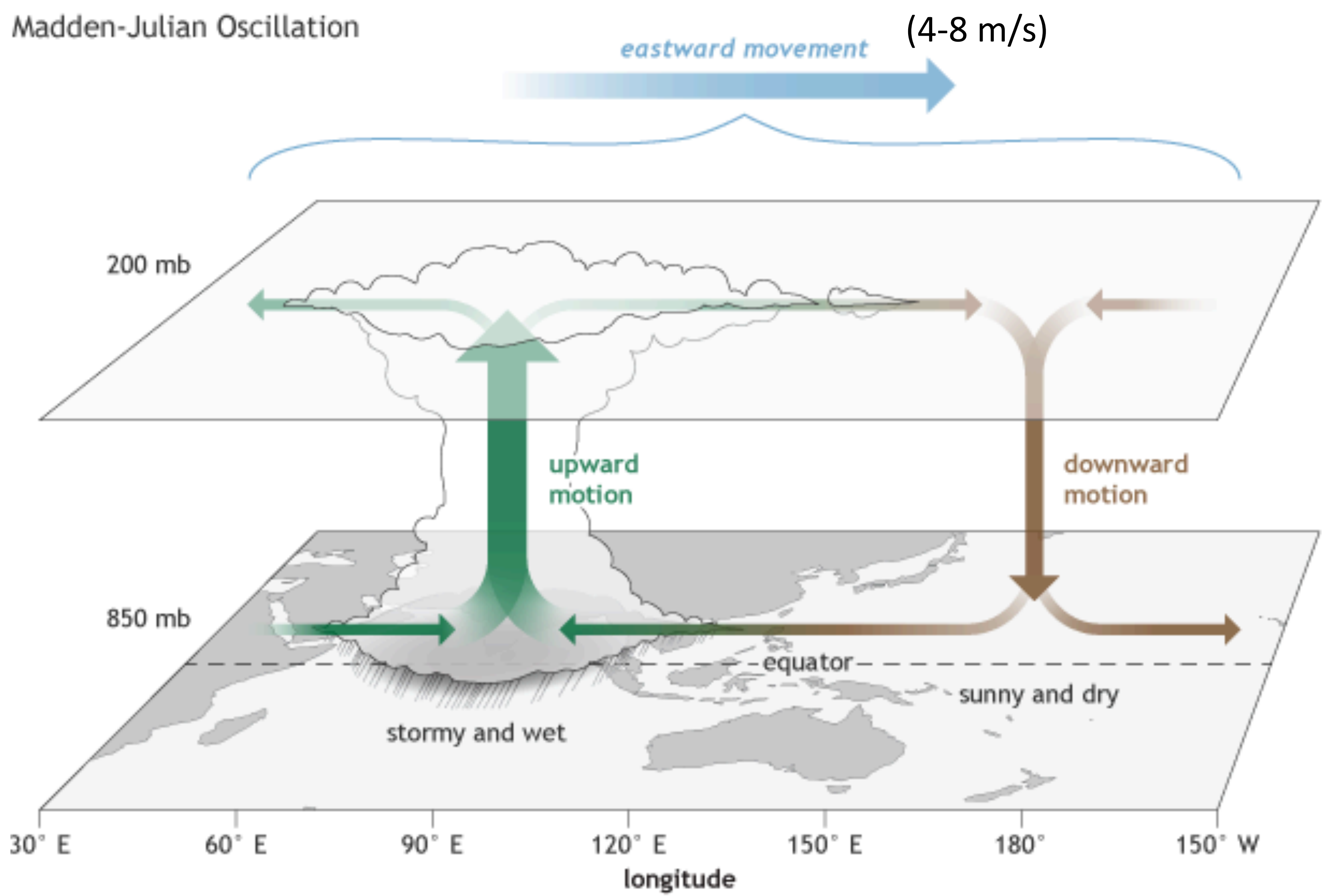

- A **pulsing of organized enhanced rainfall** that begins over the Indian Ocean
- Driven by **internal atmospheric feedbacks** – only starting to be better understood!

http://www.weathernationtv.com/news/madden-julian-oscillation-matters-winter/

Enhanced rainfall

Suppressed rainfall

8 phases of the MJO

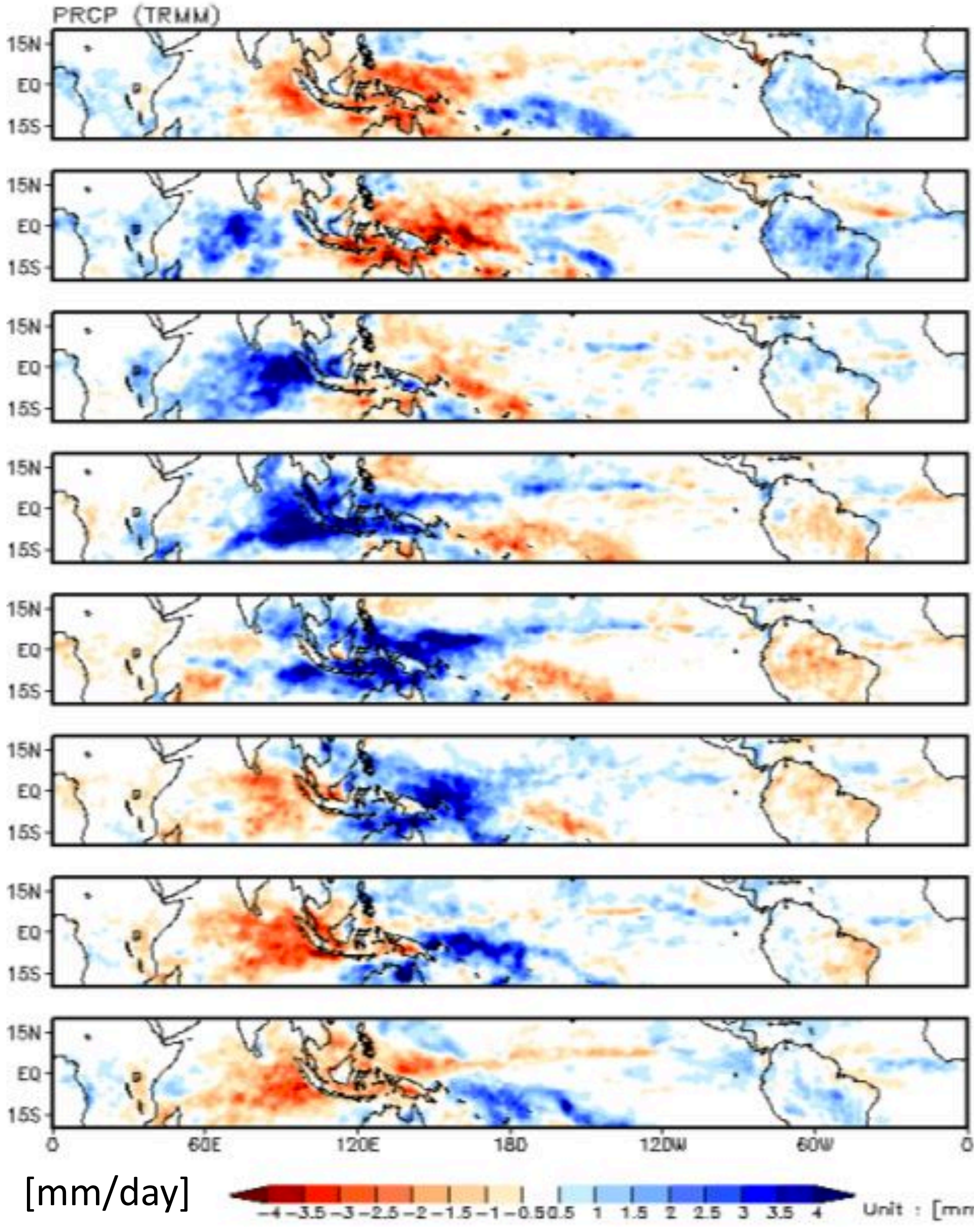

[mm/day]

Phase 1

Phase 8

time

~3 days/phase

Wheeler and Hendon (2004)

https://www.researchgate.net/figure/Composite-MJO-precipitation-anomalies-in-eight-phases-figure-courtesy-of-US-CLIVAR_fig1_255244827

Tropical OLR anomalies
15S-15N
Band-pass filtered: 15-90 day periods only

Negative OLR anomaly
(enhanced deep convective clouds)
Positive OLR anomaly
(suppressed deep convective clouds)
Contour interval = 10 W/m^2

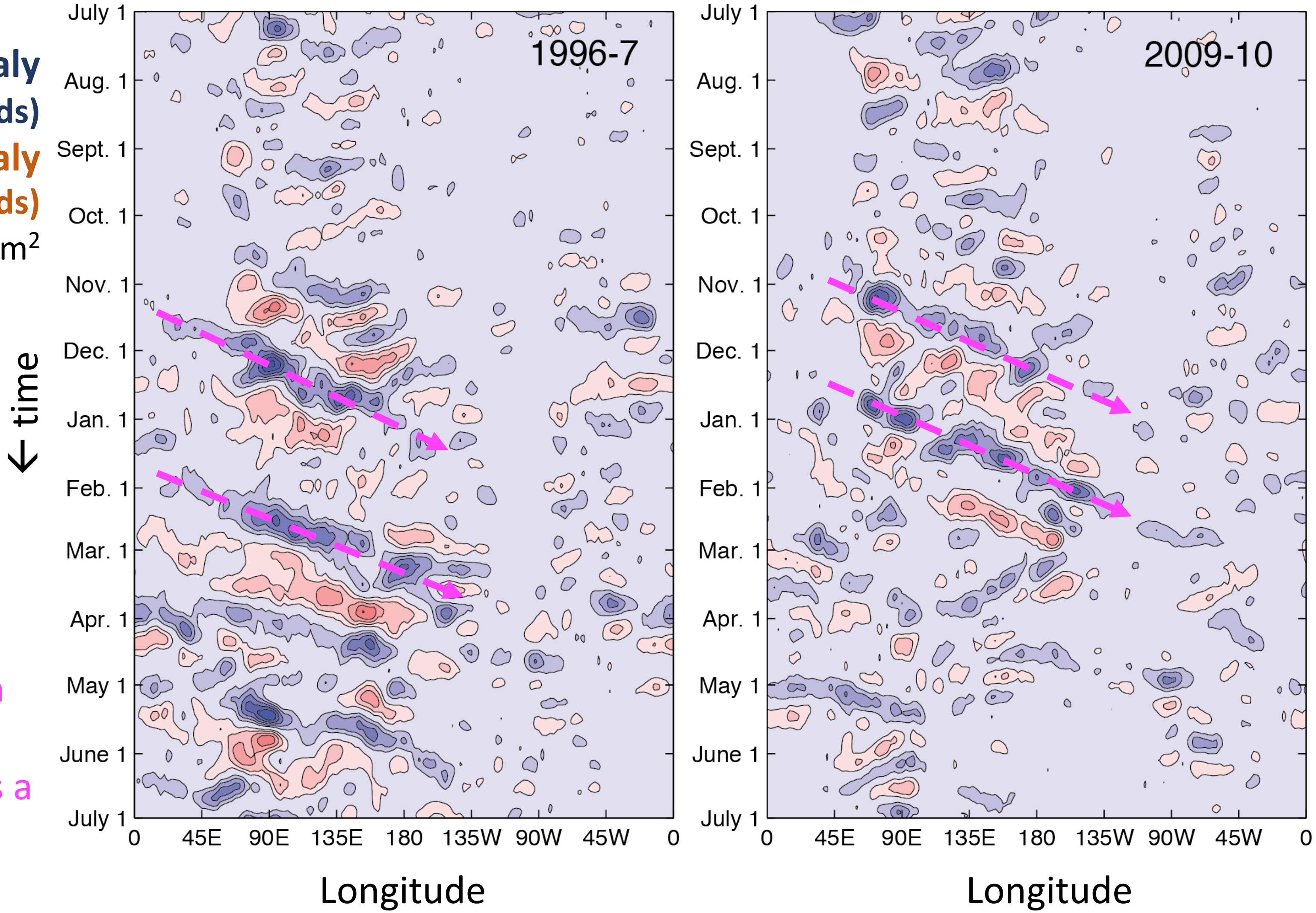

$\Delta\lambda = 180^o$ *longitude at EQ*
$\Delta t \approx 60$ *days*

$$u_{t,MJO} \approx \frac{20{,}039\ km}{5184000\ s} = +4\ m/s$$

You could think of this translation speed as a **group velocity**.
But it isn't really a true wave; it's a difficult-to-describe disturbance that moves coherently eastward.

Hartmann Fig 8.7

Negative OLR anomaly
(enhanced deep convective clouds)
Positive OLR anomaly
(suppressed deep convective clouds)
Contour interval = 2 W/m^2

Wind vector and OLR associated with 1st/2nd EOFs
of 200 hPa and 850 hPa zonal wind, Oct-Mar

First EOF (~Phase 2-3)

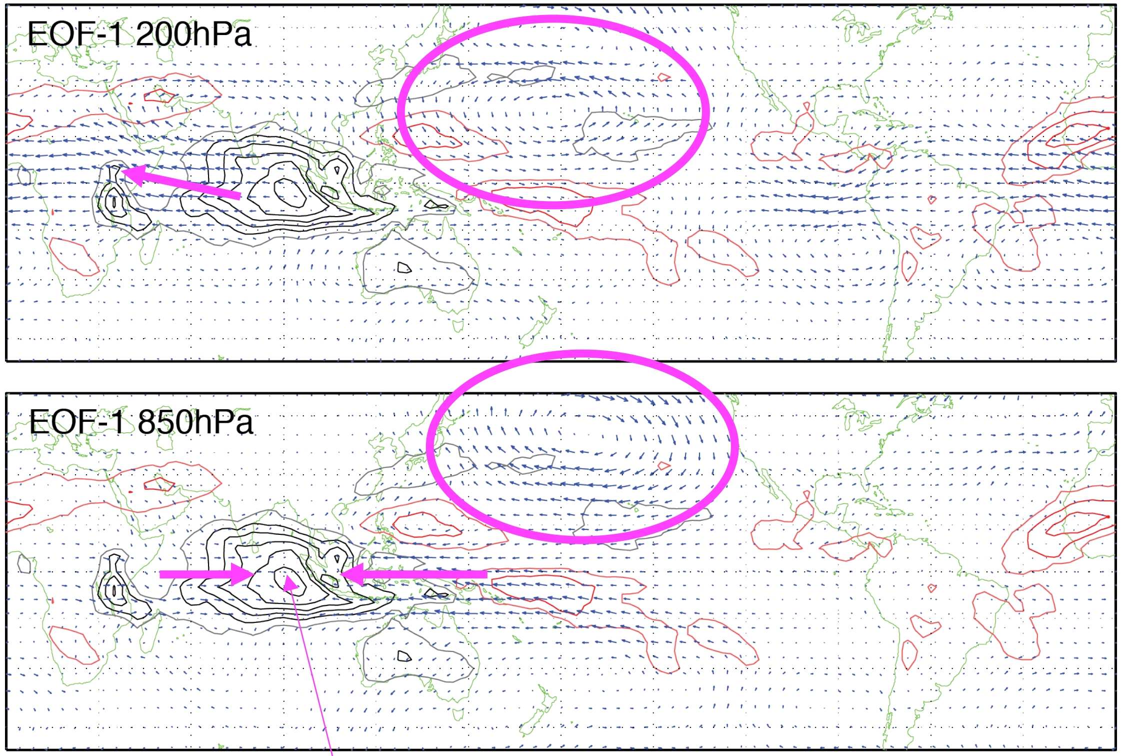

MJO enhanced precipitation

Second EOF (~Phase 4-5)

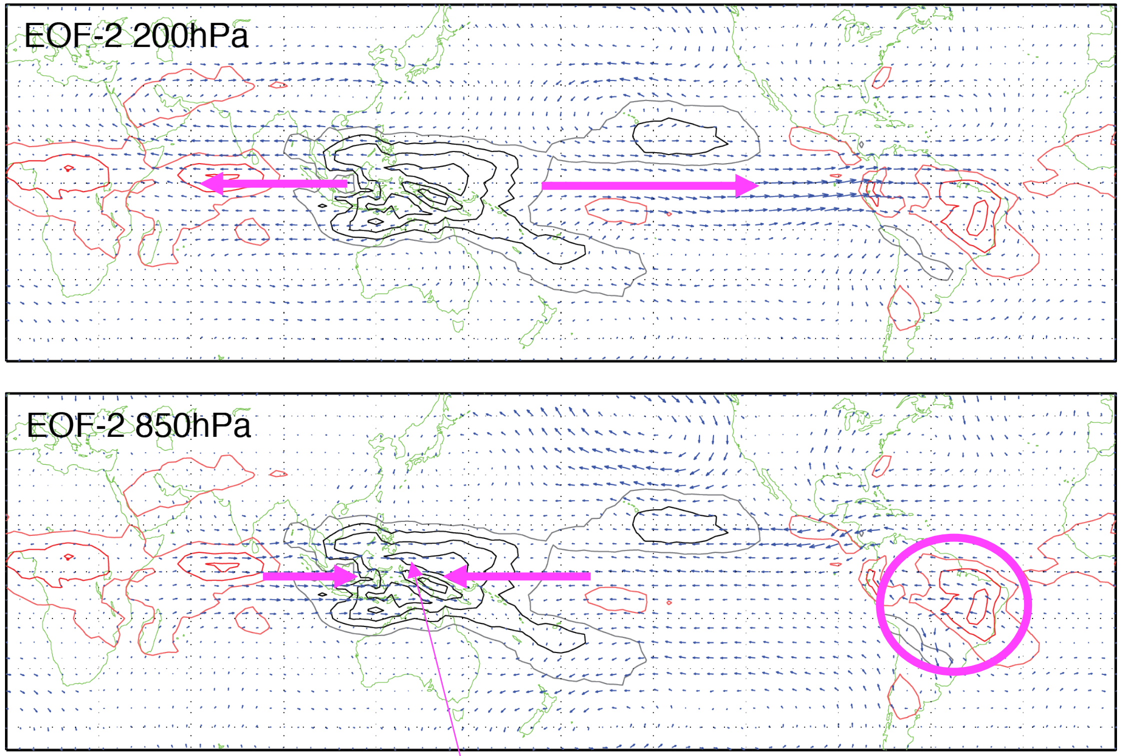

MJO enhanced precipitation

Wheeler and Hendon (2004)
Hartmann Fig 8.8

More about EOFs and their pros/cons:
https://journals.ametsoc.org/doi/pdf/10.1175/2009JCLI3062.1

Real-time daily MJO tracking
Wheeler and Hendon (2004)
MJO phase diagrams

Phase and amplitude of the MJO based on the principal component time series of the leading two EOFs from a combined EOF analysis using 850 hPa zonal wind, 200 hPa zonal wind and OLR.

Counter-clockwise movement around the diagram indicates an eastward propagating signal across eight phases from the Indian Ocean to the Pacific and later the western hemisphere.

Color of lines distinguish different months and dates are annotated.

The farther away from the center of the circle the stronger the MJO signal.

https://www.cpc.ncep.noaa.gov/products/precip/CWlink/MJO/whindex.shtml

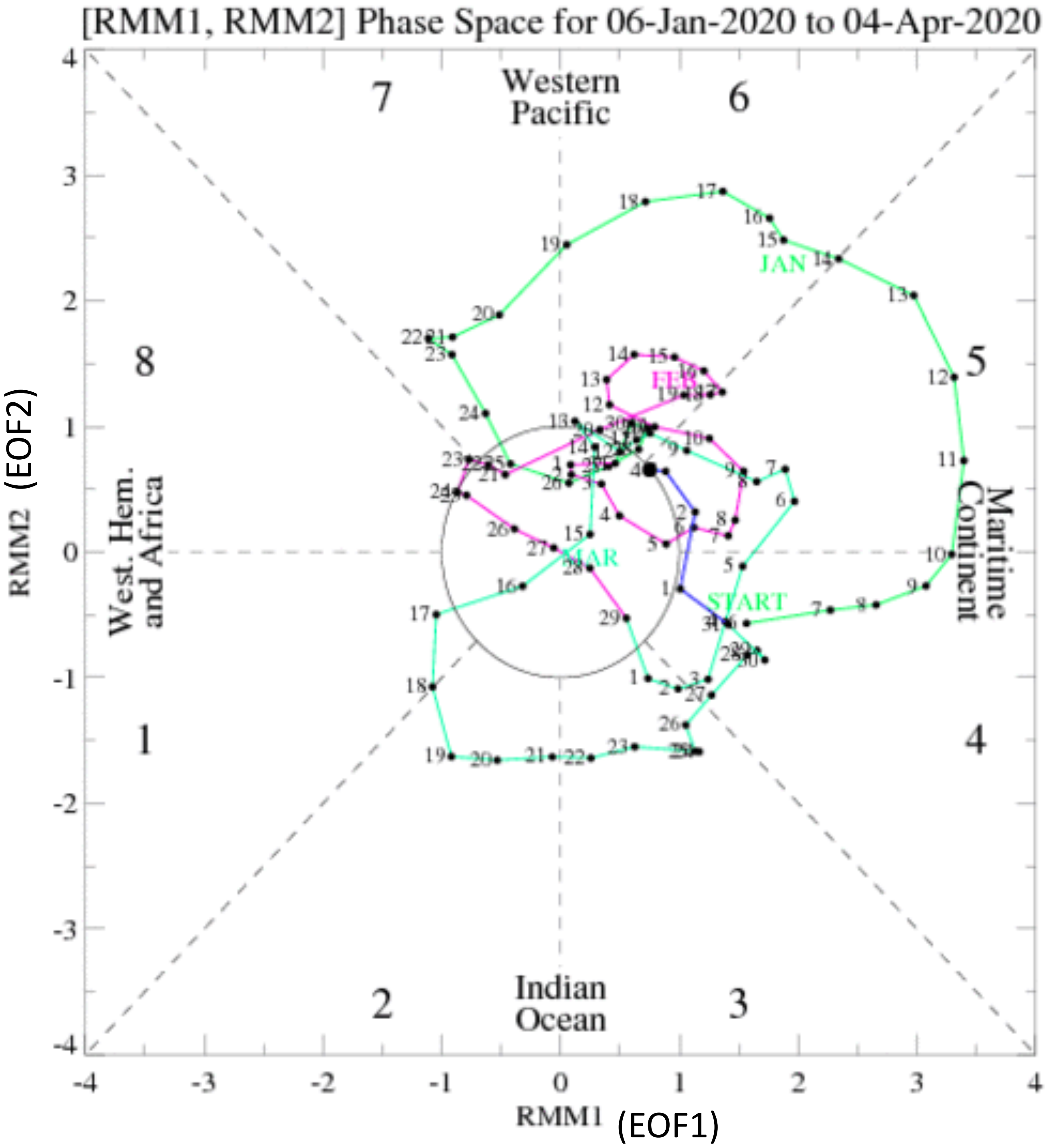

MJO teleconnections: an example

daily mean Temperature [K]

(Not all statistically significant!)

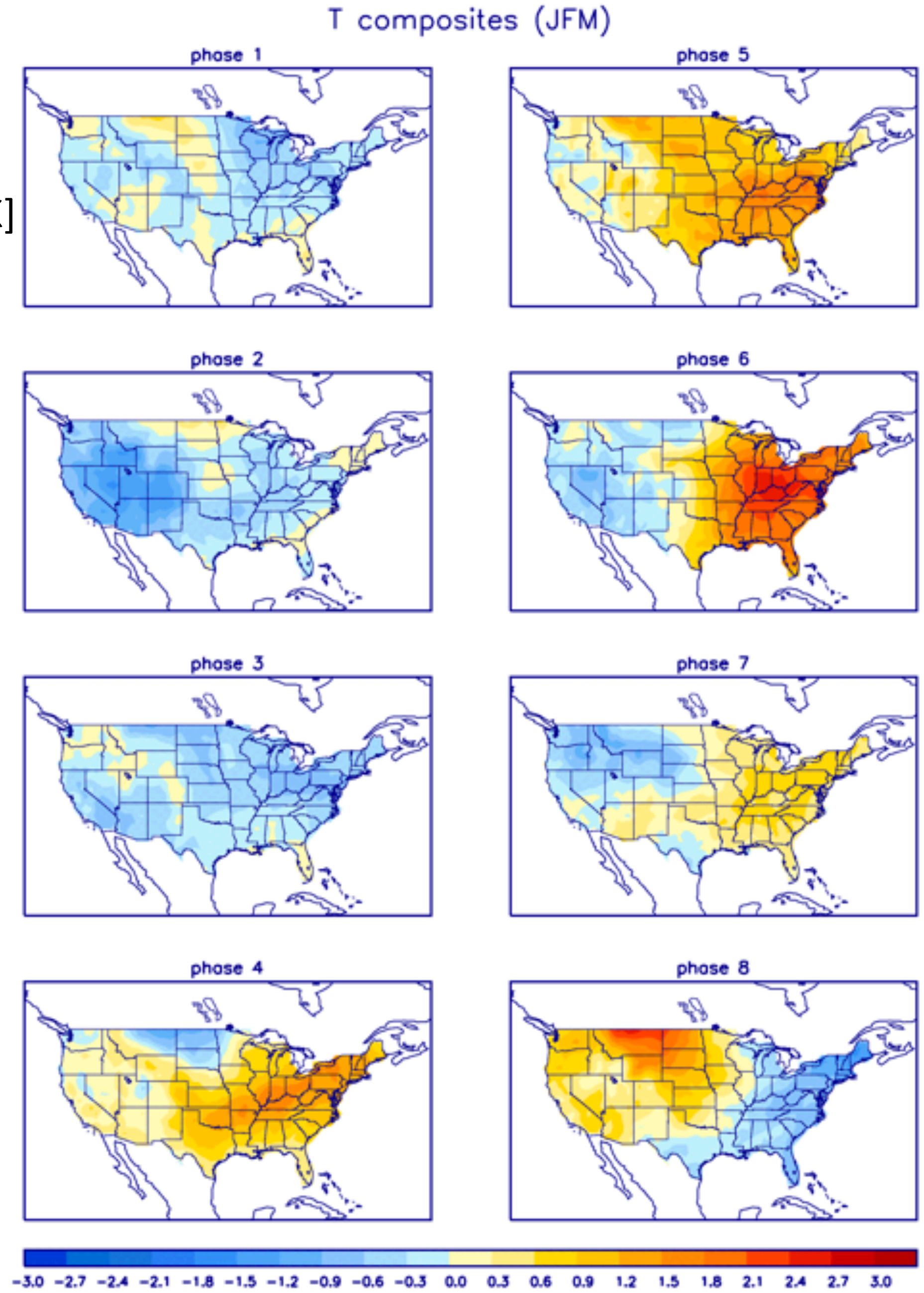

daily mean precipitation [mm/day]

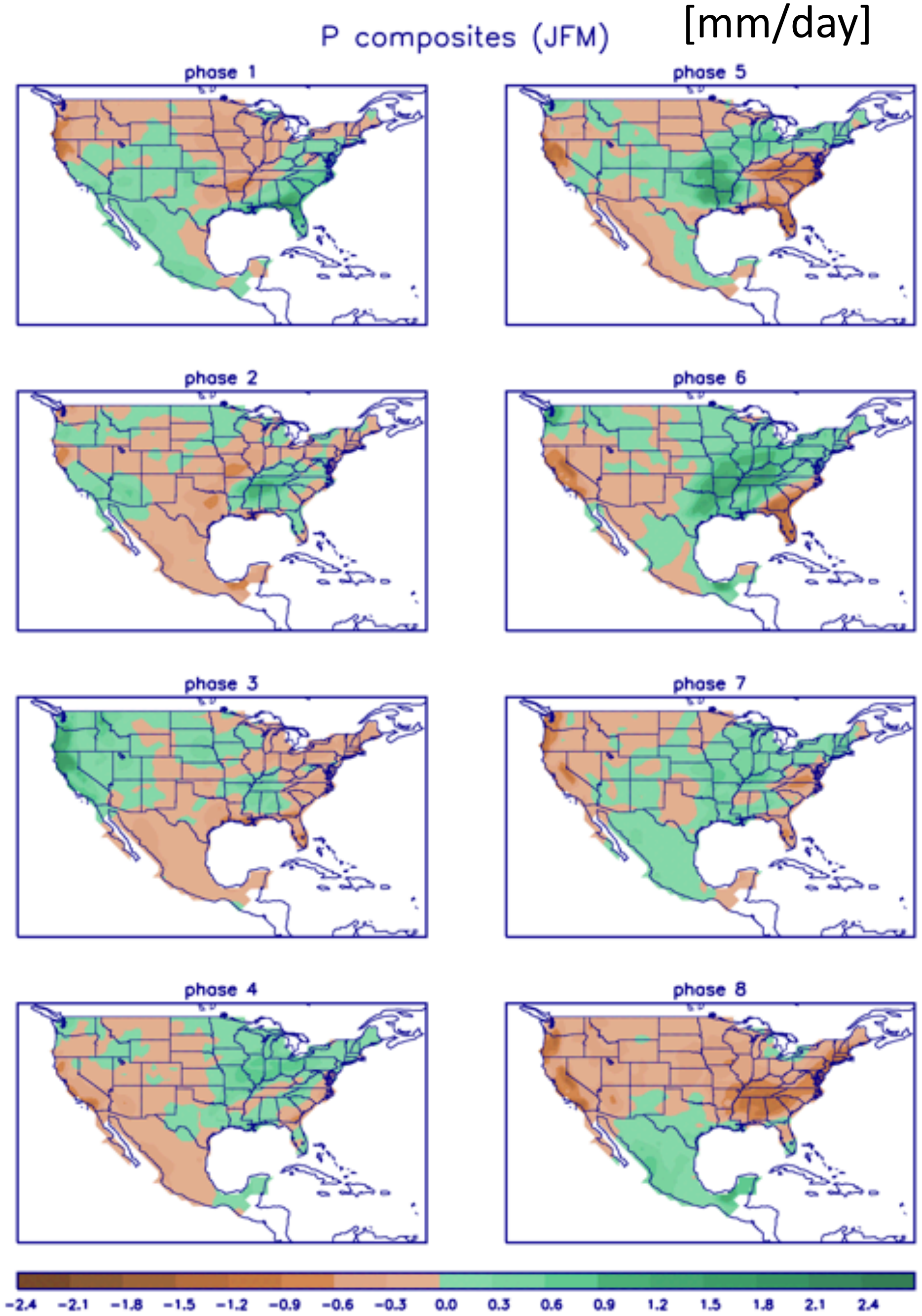

https://www.cpc.ncep.noaa.gov/products/precip/CWlink/MJO/Composites/Temperature/

Physics

If given enough time (~10s of days), convection spontaneously self-aggregates in uniform non-rotating radiative-convective equilibrium

Small domain: $L_{x,y}$ = 198 km
(Regular convection)

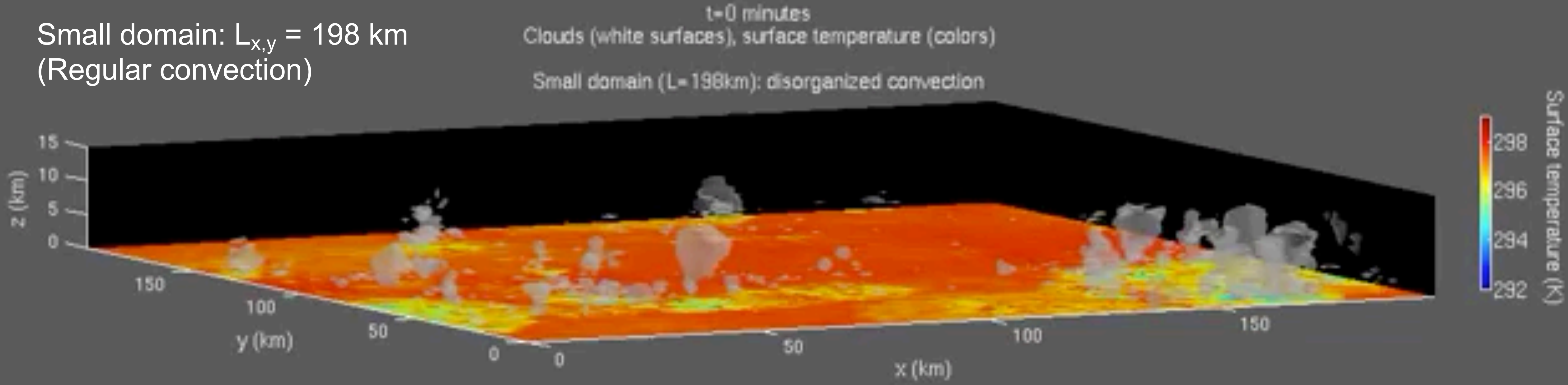

Large domain: $L_{x,y}$ = 510 km
(Aggregated convection)

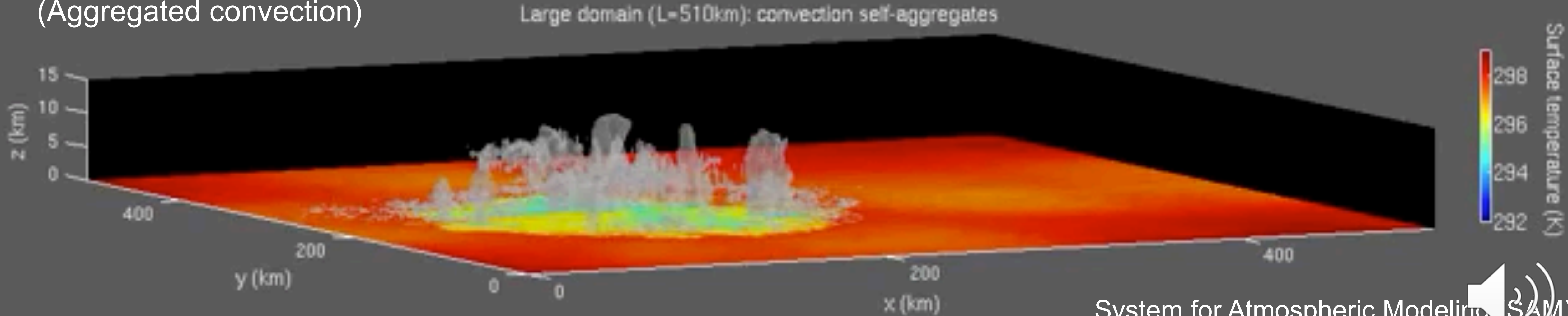

System for Atmospheric Modeling (SAM)
white contours = isosurfaces of condensate amounts (liquid and ice)

https://www.youtube.com/watch?v=chIzYtJjxhc

What creates the MJO and why does it move eastward?

Khairoutdinov and Emanuel (2018, JAS)

How an MJO forms and moves an aquaplanet without SST gradients

Recent studies have suggested that the Madden–Julian oscillation is a result of an instability driven mainly by cloud–radiation feedbacks, similar in character to self-aggregation of convection in nonrotating, cloud-permitting simulations of radiative–convective equilibrium (RCE). Here we bolster that inference by simulating radiative–convective equilibrium states on a rotating sphere with constant sea surface temperature, using the cloud-permitting System for Atmospheric Modeling (SAM) with 20-km grid spacing and extending to walls at 46° latitude in each hemisphere. Mechanism-denial experiments reveal that cloud–radiation interaction is the quintessential driving mechanism of the simulated MJO-like disturbances, but wind-induced surface heat exchange (WISHE) feedbacks are the primary driver of its eastward propagation. WISHE may also explain the faster Kelvin-like modes in the simulations. These conclusions are supported by a linear stability analysis of RCE states on an equatorial beta plane.

Khairoutdinov, M.F. and Emanuel, K., 2018. Intraseasonal variability in a cloud-permitting near-global equatorial aquaplanet model. *Journal of the Atmospheric Sciences*, *75*(12), pp.4337-4355.

“Aquaplanet” – no land
SST = 300K *everywhere*

“Near-global” domain: 46S-46N

Meridional boundaries: solid walls, free-slip

Zonal boundaries: periodic

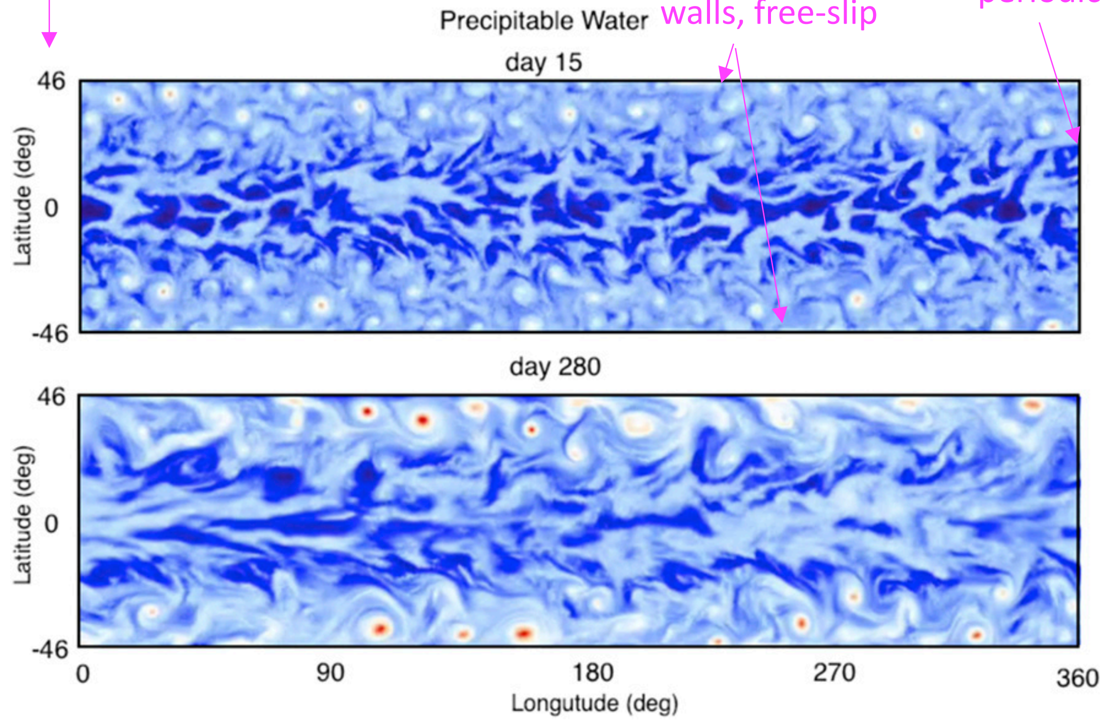

FIG. 2. Snapshots of column-integrated water vapor on (top) day 15 and (bottom) day 280.

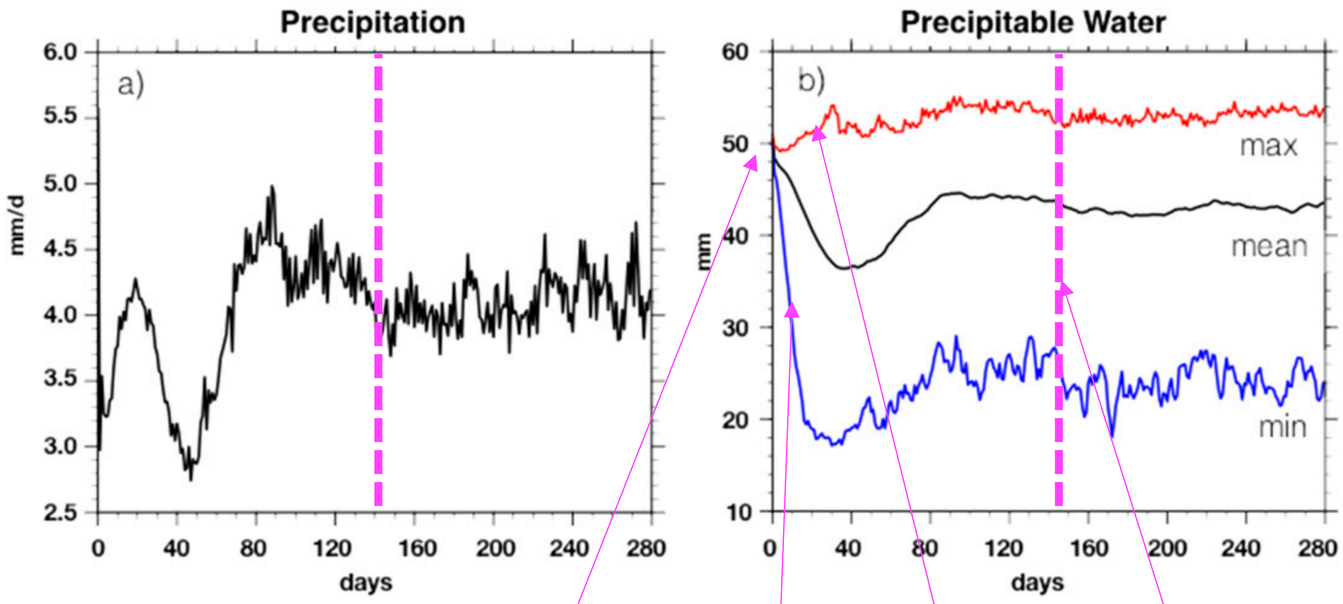

FIG. 1. Time evolution of (a) precipitation rate and (b) mean (black), minimum (blue), and maximum (red) precipitable water.

Initially nearly uniform

Dry regions form first

Moist convecting regions form next

System reaches a statistical equilibrium

Moist region
(enhanced convection)

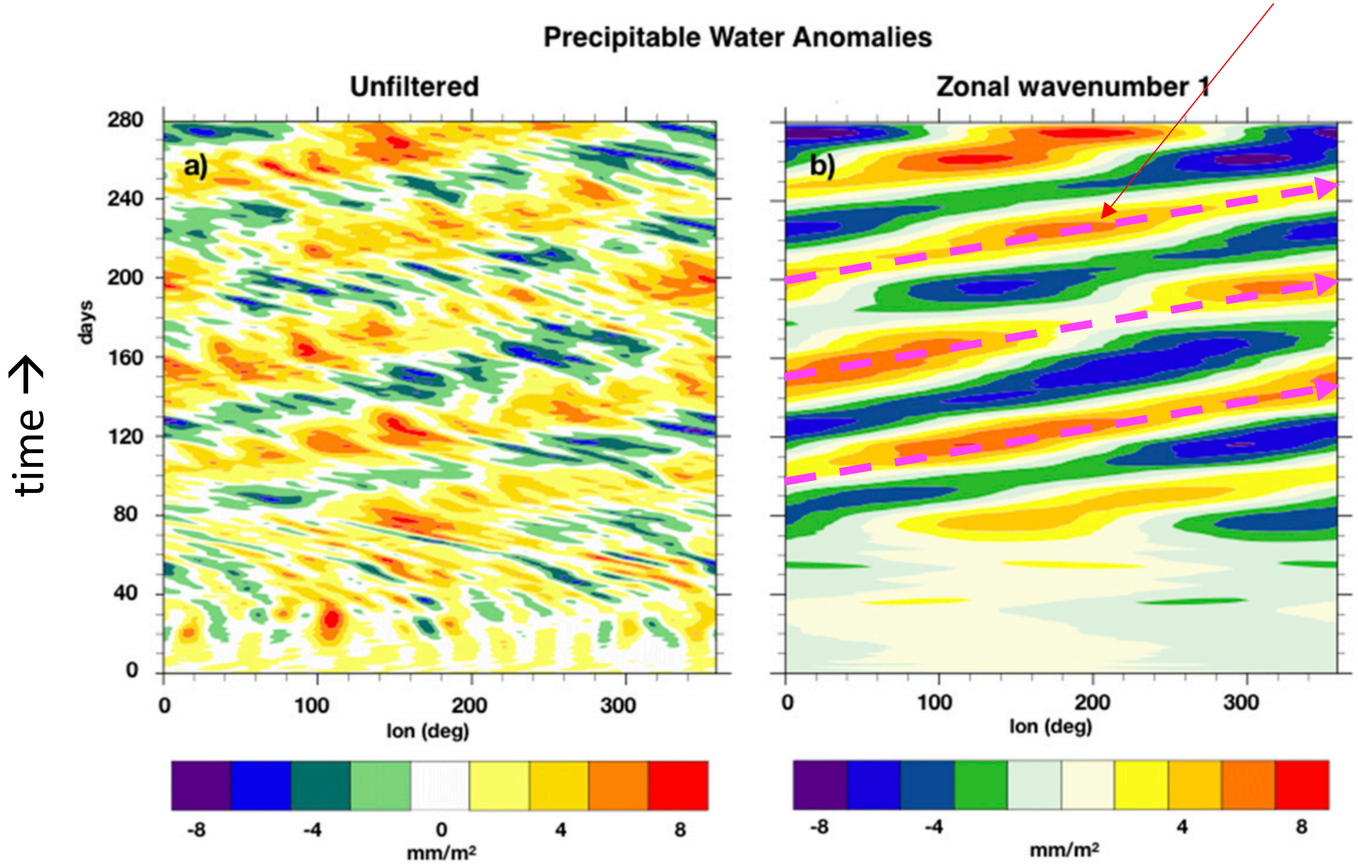

FIG. 4. Hovmöller diagram of equatorial (10°S–10°N) precipitable water anomalies in the CTRL simulation for (a) unfiltered and (b) only zonal wavenumber-1 mode remaining.

This is one continuous propagating disturbance!

$$\tau_{circumnavigate} \approx 60\ days$$
$$u_t \approx +8\ m/s$$

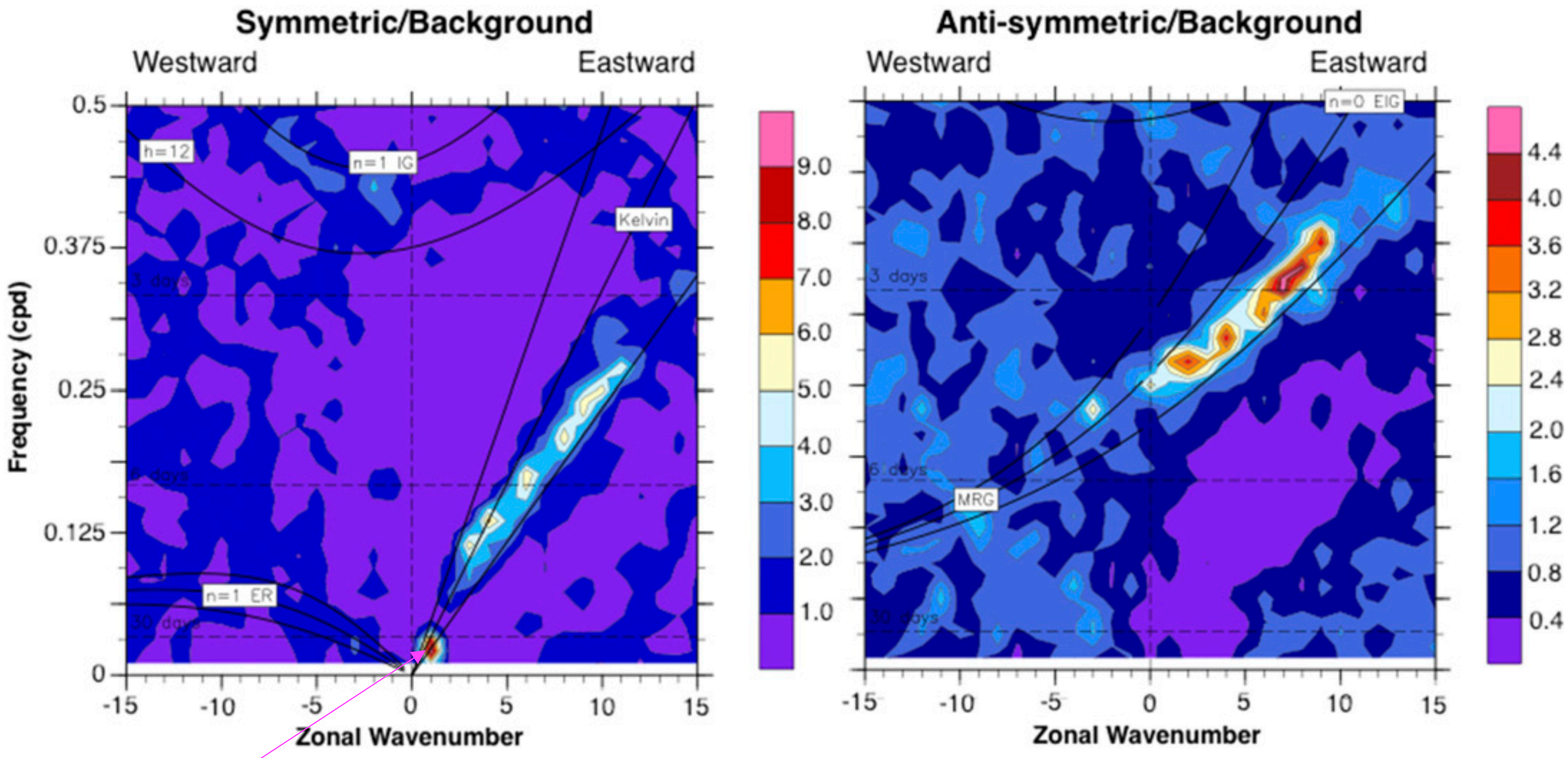

FIG. 5. Wavenumber–frequency (left) symmetric and (right) antisymmetric spectra about the equator of OLR over the equatorial belt (10°S–10°N). The ratio of the total power over the background power is shown. The thin lines represent the 12-, 25-, and 50-m equivalent depth of shallow-water theory.

MJO spectral signature

Some signs of a Matsuno-Gill type response as well

Equatorial Kelvin wave extension to east

Off-equatorial Rossby wave extension to west

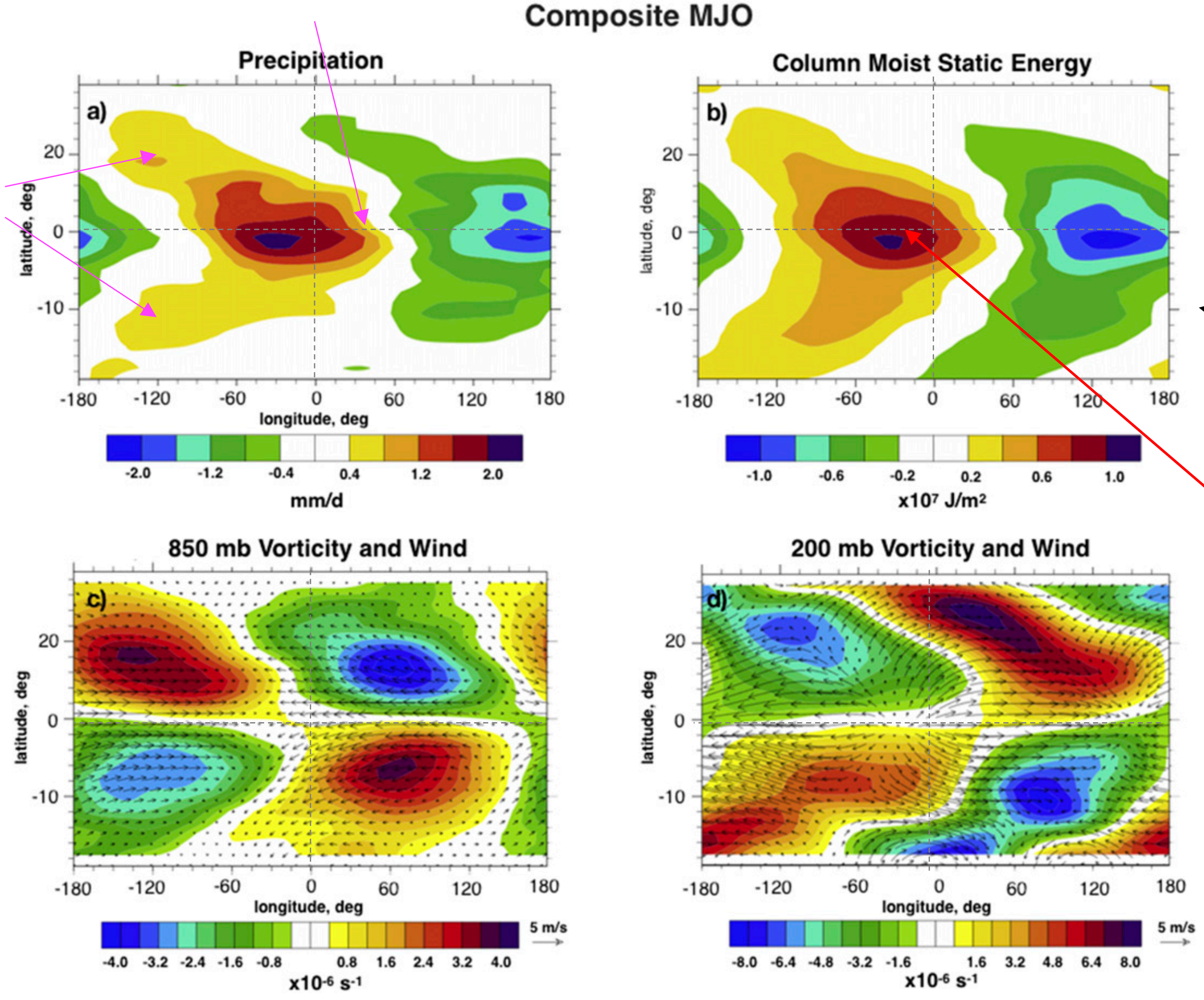

FIG. 7. Anomalies for the composite MJO-like disturbance with zonal wavenumbers larger than 4 filtered out for (a) precipitation rate, (b) column MSE, and relative vorticity with corresponding wind at (c) 850 and (d) 200 hPa.

$$m = gz + C_p T + L_v r_v$$

(they use m instead of h)

Column-integrated MSE:

$$\langle m \rangle = -\frac{1}{g}\int_{p_{sfc}}^{0} m\, dp$$

MJO is a region of enhanced moisture (and precipitation) – i.e. high column MSE

What can change $\langle m \rangle$?

$$m = gz + C_p T + L_v r_v$$

$$\langle m \rangle = -\frac{1}{g}\int_{p_{sfc}}^{0} m\, dp$$

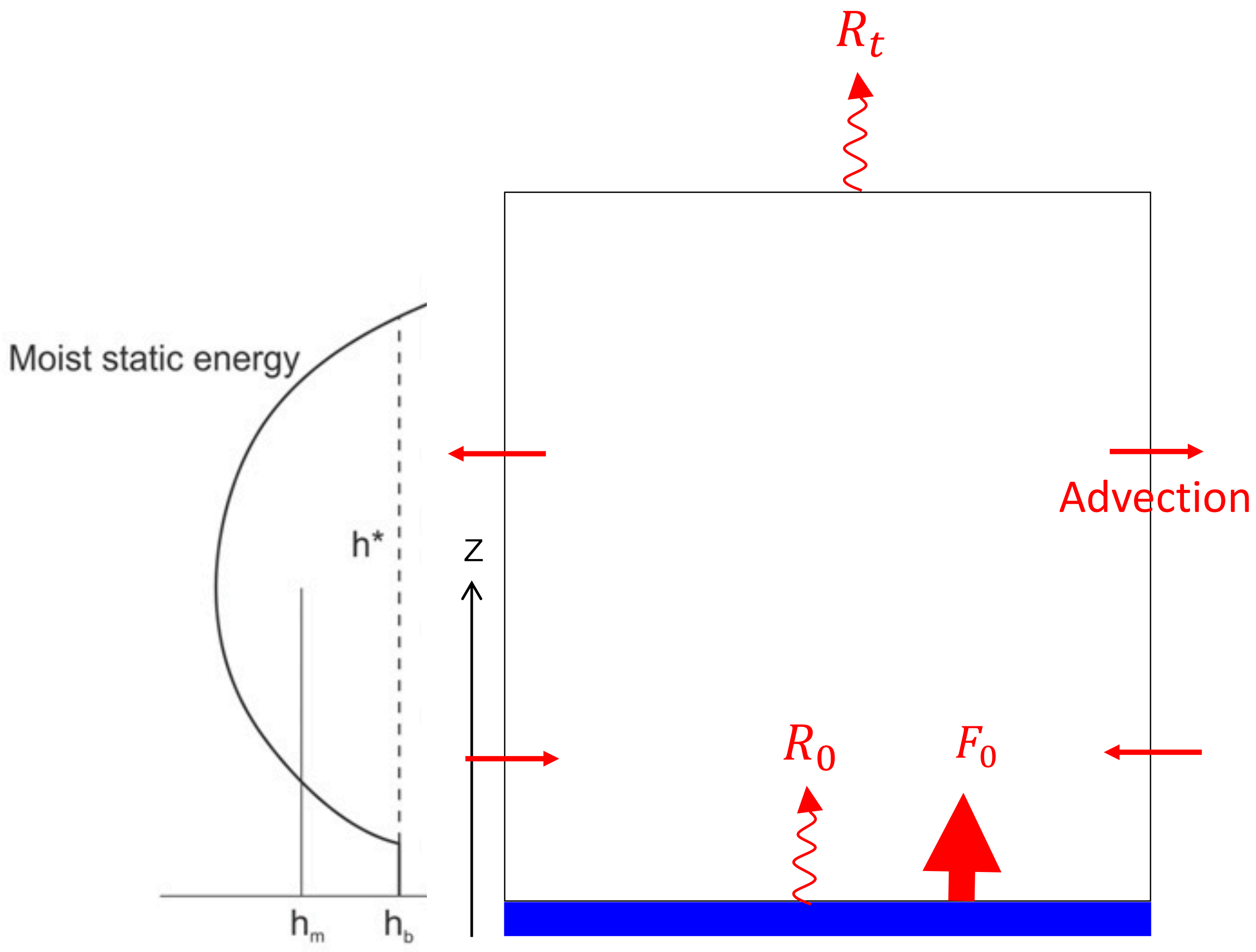

Budget equation for column-integrated MSE

$$\frac{\partial \langle m \rangle}{\partial t} = \underbrace{-c\frac{\partial \langle m \rangle}{\partial x} - \langle \mathbf{V}\cdot\nabla m\rangle - \left\langle \omega \frac{\partial m}{\partial p}\right\rangle}_{\text{Advection}} + F_0 + \underbrace{R_0 - R_t}_{\text{Net radiative heating}}. \quad (2)$$

They separate out the translation speed of the MJO itself

Surface enthalpy fluxes (latent + sensible heat)

Upward radiative flux from surface

Upward radiative flux out top of atmos

Left fig from Emanuel (2019, JAS)

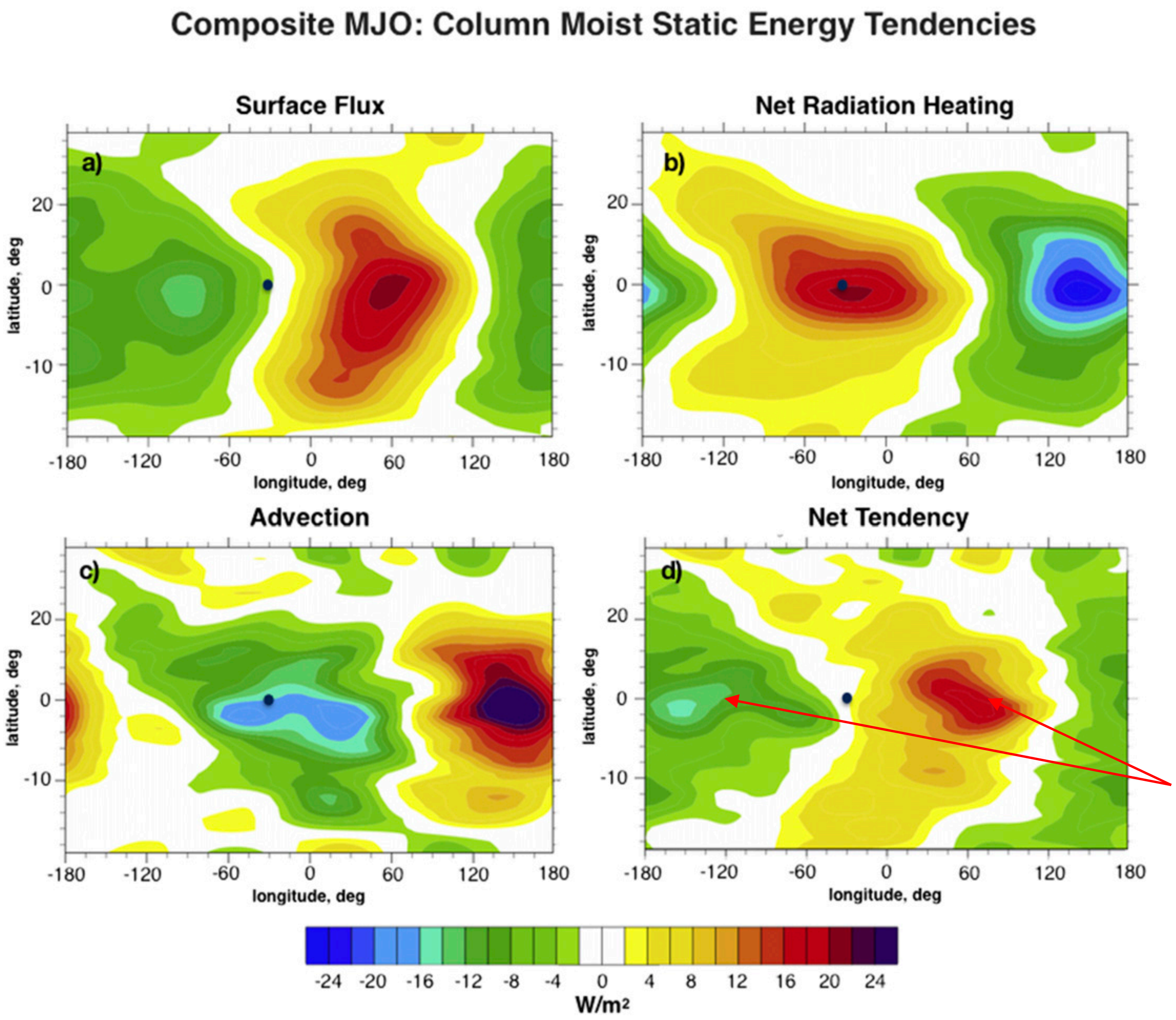

FIG. 8. Composite budget of the column-integrated MSE tendencies for the composite MJO-like disturbance in the CTRL simulation due to (a) surface enthalpy flux, (b) net radiation heating, (c) advection of MSE, and (d) net local tendency due to all processes. The center of MJO-like disturbance is marked by a dot.

Budget equation for column-integrated MSE

$$\frac{\partial\langle m\rangle}{\partial t} = \underbrace{-c\frac{\partial\langle m\rangle}{\partial x} - \langle \mathbf{V}\cdot\nabla m\rangle - \left\langle \omega\frac{\partial m}{\partial p}\right\rangle}_{\text{Advection}} + F_0 + \underbrace{R_0 - R_t}_{\text{Net radiative heating}}. \qquad (2)$$

Surface enthalpy fluxes

Net tendency $\frac{\partial\langle m\rangle}{\partial t}$ is positive to the east and negative to the west of current center – **the moist region will propagate eastward**

Composite MJO: Column Moist Static Energy Tendencies

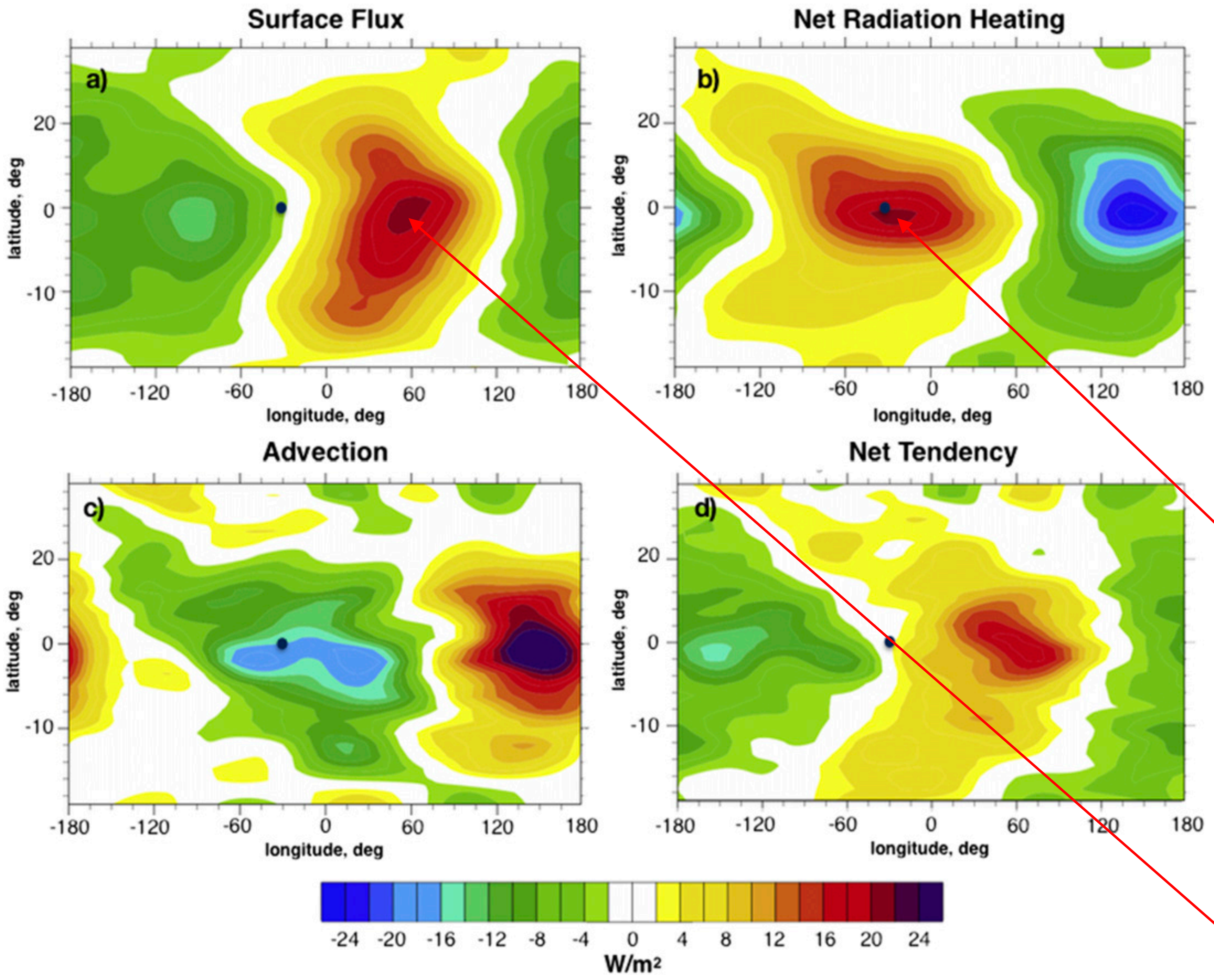

FIG. 8. Composite budget of the column-integrated MSE tendencies for the composite MJO-like disturbance in the CTRL simulation due to (a) surface enthalpy flux, (b) net radiation heating, (c) advection of MSE, and (d) net local tendency due to all processes. The center of MJO-like disturbance is marked by a dot.

Budget equation for column-integrated MSE

$$\frac{\partial\langle m\rangle}{\partial t} = \underbrace{-c\frac{\partial\langle m\rangle}{\partial x} - \langle \mathbf{V}\cdot\nabla m\rangle - \left\langle \omega\frac{\partial m}{\partial p}\right\rangle}_{\text{Advection}} + F_0 + \underbrace{R_0 - R_t}_{\text{Net radiative heating}}. \quad (2)$$

Surface enthalpy fluxes

1) Net radiative heating increases $\langle m\rangle$ over MJO center (where $\langle m\rangle$ is already large) – a positive feedback that **maintains the MJO**.
Physically: more clouds/moisture = stronger greenhouse effect

2) Surface fluxes increase $\langle m\rangle$ to the east of the MJO – a feedback that **causes it to propagate eastward**.
Physically: surface fluxes increase with wind speed, and surface wind speeds are strongest to the east (easterly inflow + background equatorial easterlies)

"Mechanism-denial experiments"

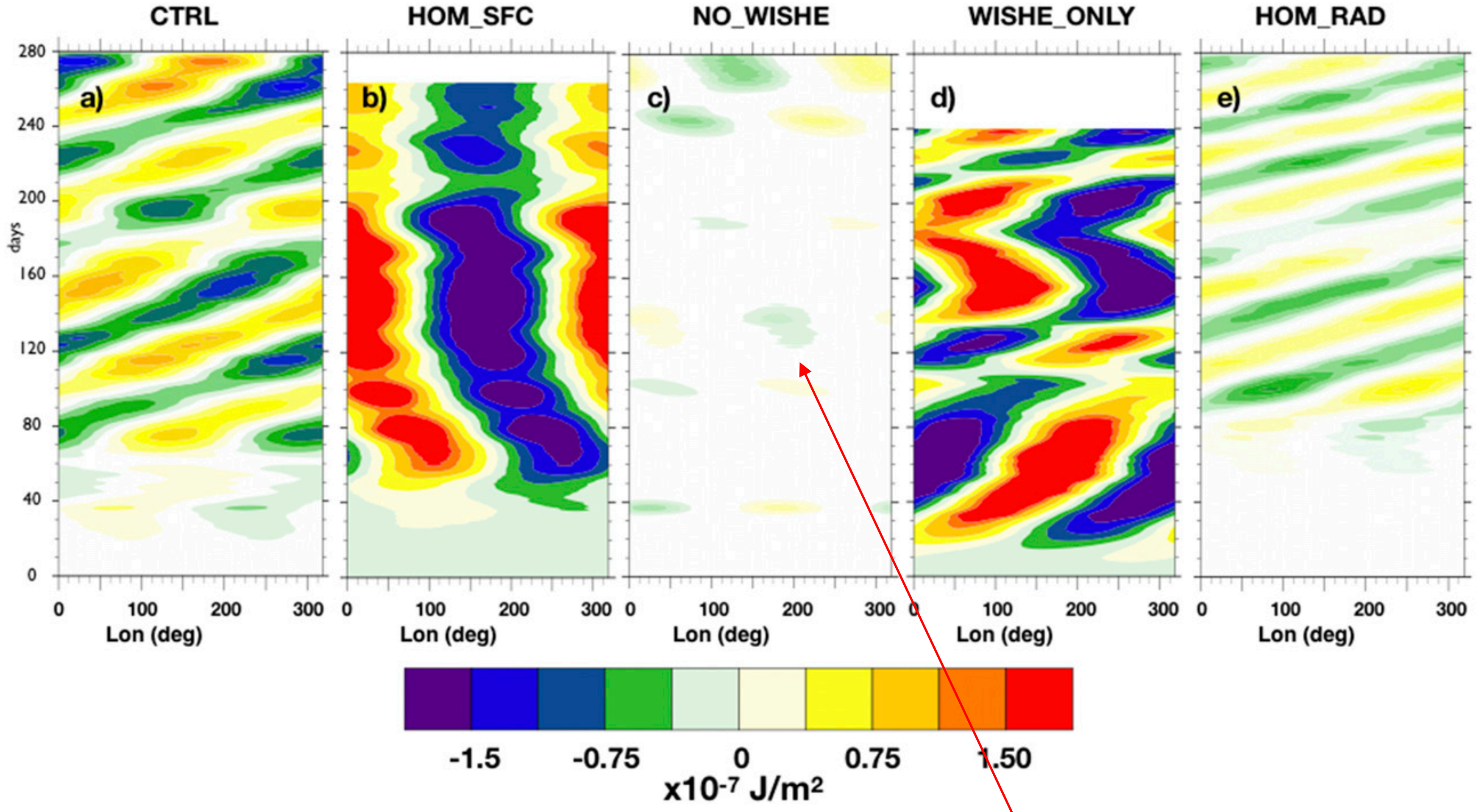

FIG. 9. Hovmöller diagrams of equatorial (10°S–10°N) zonal wavenumber-1-filtered OLR anomalies in CTRL and various mechanism-denial experiments (see text for acronyms).

Surface enthalpy flux equation: $F_0 = \rho C_k |\boldsymbol{V}| (k_{sfc}^{*} - k_{2m})$

"Wind speed induced surface-heat exchange feedback" (WISHE)

What if you simply turn this wind-speed dependence off?

(By setting $|\boldsymbol{V}| = \overline{|\boldsymbol{V}|}$ constant everywhere)

No more MJO!

“Mechanism-denial experiments”

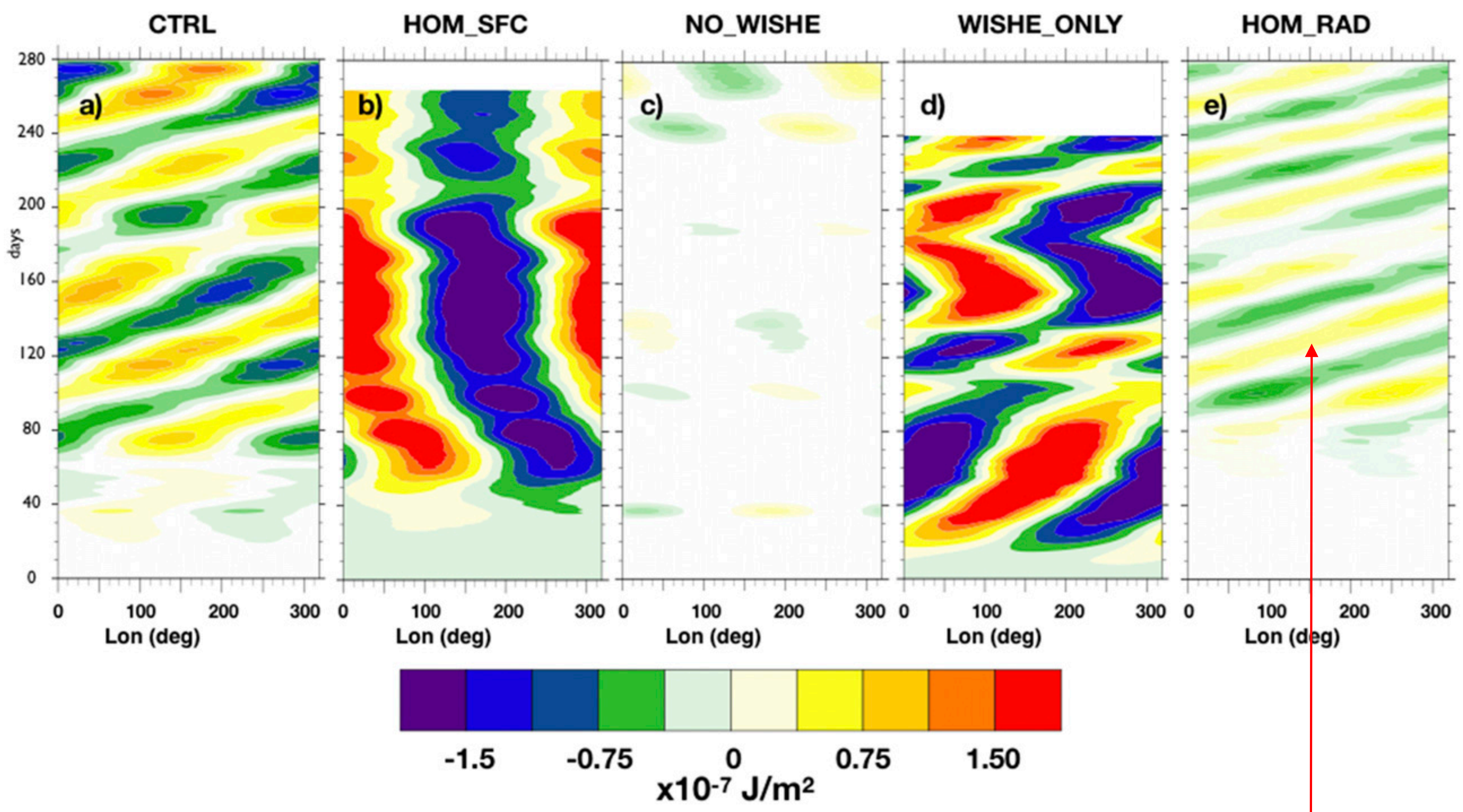

FIG. 9. Hovmöller diagrams of equatorial (10°S–10°N) zonal wavenumber-1-filtered OLR anomalies in CTRL and various mechanism-denial experiments (see text for acronyms).

What if you do not allow radiative feedbacks?

(By setting $\dot{Q}(z) = \overline{\dot{Q}(z)}$ constant everywhere,

Weaker MJO! Similar translation speed

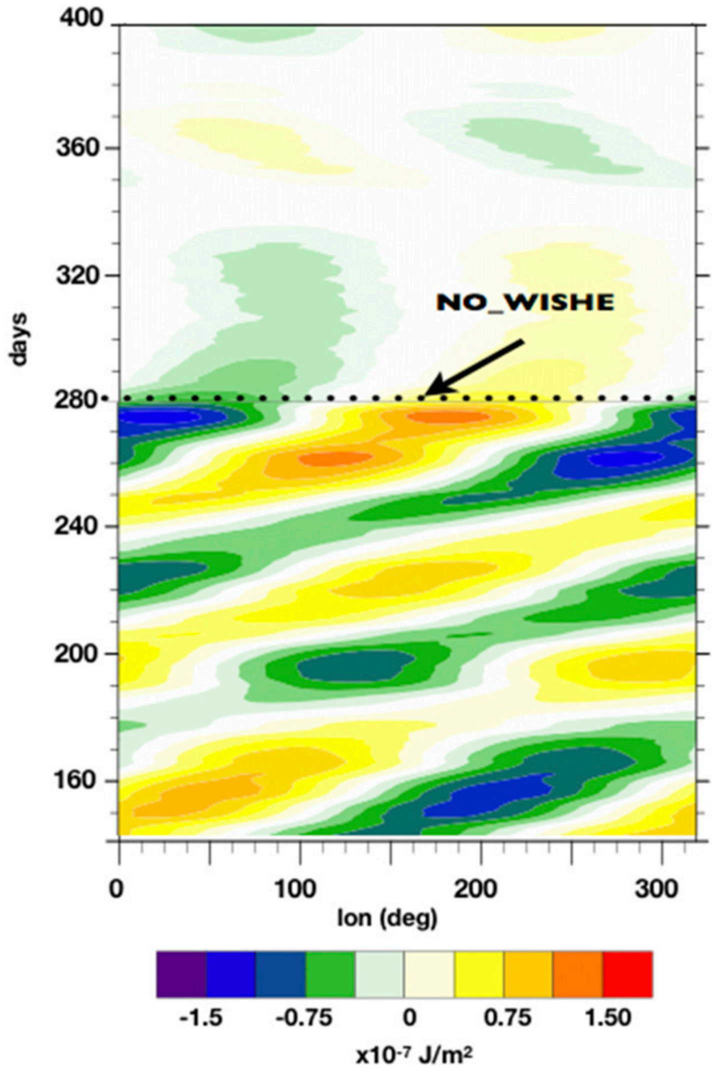

FIG. 11. Hovmöller diagrams of equatorial (10°S–10°N) zonal wavenumber-1-filtered OLR anomalies in the CTRL case interrupted at day 280 by homogenization of the surface wind speed in surface enthalpy flux computations (similar to the NO_WISHE case).

More proof that WISHE is really fundamental.
Instantaneously turn off wind-speed dependence of surface fluxes.
MJO stops moving, nearly disappears.

The MJO is not itself a unique wave mode.

It can look like a wave because it propagates. But it’s probably better thought of simply as a coherent disturbance.

It is a disturbance that emerges from slow (O(10 day)) feedbacks between moisture, radiation, and circulation.

For more information

+

a remarkable *analytical* solution for this MJO-like disturbance

Khairoutdinov, M.F. and Emanuel, K., 2018. Intraseasonal variability in a cloud-permitting near-global equatorial aquaplanet model. *Journal of the Atmospheric Sciences*, *75*(12), pp.4337-4355.

Now go to Blackboard to answer a few questions about this topic!